Congenital hypogonadotropic hypogonadism in a patient with a de novo POGZ mutation

Eskici, Nazli

Oxford University Press
2023-08-02

Eskici, N, Madhusudan, S, Vaaralahti, K, Yellapragada, V, Gomez-Sanchez, C, Kärkinen, J, Almusa, H, Brandstack, N, Miettinen, P J, Wang, Y & Raivio, T 2023, 'Congenital hypogonadotropic hypogonadism in a patient with a de novo POGZ mutation', European Journal of Endocrinology, vol. 189, no. 2, pp. 271-280. https://doi.org/10.1093/ejendo/lvad111

http://hdl.handle.net/10138/584911
10.1093/ejendo/lvad111

unspecified
acceptedVersion

Congenital hypogonadotropic hypogonadism in a patient with a de novo *POGZ* mutation

Nazli Eskici[1, 2], Shrinidhi Madhusudan[1, 2], Kirsi Vaaralahti[1,2], Venkatram Yellapragada[1, 2], Celia Gomez-Sanchez[1, 2], Juho Kärkinen[3], Henrikki Almusa[4], Nina Brandstack[5], Päivi J. Miettinen[3], Yafei Wang[1, 2]* & Taneli Raivio[1,2,3]*

[1] Stem Cells and Metabolism Research Program (STEMM), Faculty of Medicine, 00014 University of Helsinki, Helsinki, Finland; [2] Medicum, Faculty of Medicine, 00014 University of Helsinki, Helsinki, Finland; [3] Helsinki University Hospital, New Children's Hospital, Pediatric Research Center, Helsinki 00014, [4]Finland, Institute for Molecular Medicine Finland, FIMM, University of Helsinki, Helsinki, Finland, [5]Department of Radiology, Helsinki University Hospital and University of Helsinki, Helsinki, Finland

* Contributed equally

Corresponding authors: Taneli Raivio, taneli.raivio@helsinki.fi, Biomedicum Helsinki, Haartmaninkatu 8 00290 Helsinki, FINLAND

Keywords: Congenital hypogonadotropic hypogonadism, Kallmann syndrome, POGZ, GnRH neurons, puberty

Running head: *POGZ* mutation in Kallmann syndrome

ABSTRACT

Objective: Congenital hypogonadotropic hypogonadism (CHH) is a rare, genetically heterogeneous reproductive disorder caused by gonadotropin-releasing hormone (GnRH) deficiency. Approximately half of CHH patients also have decreased or absent sense of smell, *i.e.* Kallmann syndrome (KS). We describe a patient with White-Sutton syndrome (developmental delay and autism spectrum disorder) and KS due to a heterozygous *de novo* mutation in *POGZ* (c.2857C>T, p.(Gln953*)), a gene encoding pogo transposable element derived with zinc finger domain, which acts as a transcriptomic regulator of neuronal networks.

Design & Methods: We modelled the role of *POGZ* in CHH by generating two clonal human pluripotent stem cell lines with CRISPR/Cas9, carrying either the heterozygous patient mutation (H11 line), or a homozygous mutation (c.2803-2906del; p.E935Kfs*7 encoding a truncated POGZ protein; F6del line).

Results: During the differentiation to GnRH neurons, neural progenitors derived from F6del line displayed severe proliferation defect, delayed wound-healing capacity, downregulation of intermediate progenitor neuron genes *TBR1* and *TBR2* and immature neuron markers *PAX6* and *TUBB3*, and gave rise to fewer neurons with shorter neurites and less neurite branch points compared to the WT and H11 lines ($P<0.005$). Both lines, however, could be successfully differentiated to GnRH neurons.

Conclusions: In conclusion, this is the first report on the overlap between White-Sutton syndrome and CHH. *POGZ* mutations do not hinder GnRH neuron formation, but may cause CHH/KS by affecting the size and motility of the anterior neural progenitor pool, and neurite outgrowth.

Significance Statement

We report the first White-Sutton syndrome patient with a mutation in POGZ (c.2857C>T, p.(Gln953*)) who also has Kallmann syndrome (KS). POGZ deficiency in human pluripotent stem cells did not impair GnRH neurogenesis but disrupted the proliferation of neural progenitors, axon outgrowth, and branching. In conclusion, patients with POGZ mutations should be evaluated for the presence of KS.

INTRODUCTION

Congenital hypogonadotropic hypogonadism (CHH) is a clinically and genetically heterogeneous disease characterized by absent or incomplete puberty and infertility (1) together with low serum levels of sex steroids and gonadotropins (luteinizing hormone and follicle-stimulating hormone) (2). When CHH manifests with deficient sense of smell (hyposmia or anosmia), it is called Kallmann syndrome (KS). CHH/KS is caused by GnRH deficiency (1, 3). GnRH neurons are born in the olfactory placode during early embryonic development and migrate along vomeronasal nerves into the central nervous system (CNS) (4). Once they reach their final destination in the hypothalamus, they extend their projections to the median eminence where they have the capacity to release the GnRH decapeptide (3). GnRH stimulates gonadotropic cells in the anterior pituitary gland to produce and release gonadotropins that control gonadal maturation and the reproductive system (1).

Patients with CHH exhibit a wide clinical spectrum including reproductive (reduced testicular volume, absent puberty, micropenis, and cryptorchidism in males, and absent breast development, and primary amenorrhea in females) and non-reproductive (cleft lip/palate, hearing loss, synkinesia, dental agenesis) phenotypes (1, 3).

So far, mutations in 75 genes have been implicated in CHH (5-13) (Supplementary file 4) and different modes of inheritance, including oligogenecity, have been described (3, 14). The genetic complexity is reflected by varying phenotypic features due to incomplete penetrance and variable expressivity. Moreover, CHH clinically overlaps with other syndromes such as CHARGE syndrome (*CHD7* mutations) (15), Waardenburg syndrome (*SOX10* mutations) (16), Hartsfield syndrome (*FGFR1* mutations), TUBB3 E410K syndrome (recurrent heterozygous *TUBB3* E410K mutation) (17), and a syndrome caused by mutations in *DMXL2* (14, 18).

POGZ, a transcriptional regulator that promotes neuronal gene expression and chromatin accessibility, is highly expressed in the fetal and adult central nervous system (CNS) in both humans and mice (19-22) and plays an important role in neural differentiation of mouse and human stem cells (23, 24). Heterozygous loss-of-function mutations in *POGZ* cause White-Sutton syndrome (WHSUS) which is characterized by intellectual disability, and developmental delay with or without autism spectrum disorder (ASD) and dysmorphic facial features (19, 25, 26, 27). There are no reports of WHSUS patients with homozygous *POGZ* mutations, and indeed, homozygous *Pogz* mutations in mice are embryonic lethal (21).

In this paper, we describe a WHSUS patient, with a novel *de novo POGZ* mutation, who also has CHH and KS. To investigate the mechanism underlying the CHH phenotype, we generated two different *POGZ* mutation lines in hESCs. We introduced the patient' s heterozygous mutation in one line and a homozygous deletion leading to truncated protein in another line and investigated their ability to differentiate into anterior neurons using our GnRH neuron differentiation protocol (28-31). Our results demonstrate that POGZ is required for the formation of the anterior neural progenitor pool and that the absence of full-length POGZ impairs neurite outgrowth and branching of anterior neurons. These results suggest that POGZ is not indispensable for GnRH neuron ontogeny but may cause CHH/KS by affecting the size and motility of the anterior neural progenitor pool, and neurite outgrowth.

PATIENTS AND METHODS

Patient description

The index patient was born following a full-term pregnancy (birth weight 3440 g /birth length 52 cm /head circumference 33 cm). After birth, he was diagnosed with micropenis (length 13 mm) with normally descended testes. He had abnormal shape of L1 to L3, L5 and C2 and C3 vertebrae. At the age of 0 and 1 month, he received two doses of intramuscular testosterone 25mg (Testoviron®) with a good response in penile growth (from 13 to 29 mm). At the age of 6 months, the patient underwent GnRH stimulation test. His basal LH level was <0.1 IU/L and peak LH was 3.6 IU/L. Both values were below the reported values in

healthy boys (32, 33). Ophthalmologist diagnosed bilateral astigmatismus and optic nerve atrophy. Olfactory bulbs were not visible in his brain MRI, obtained at the age of 8 months, though olfactory sulci were present; anterior pituitary was small (Fig.1). Developmental delay (motor delay, speech delay, intellectual disabilities, and learning difficulties) of unknown etiology was noted from early on. He also had microcephaly (head circumference -4.3 SDS at the age 5 years), brachycephaly, frontal bossing, hypertelorism, downslanting palpebral fissures, midface hypoplasia, flat nasal bridge, anteverted nares, triangular mouth, high-arched palate, abnormally folded and posteriorly-rotated ears, autism, constipation, diarrhea, cyclic vomiting, and reflux, all of which are common WHSUS features (27). His electroencephalography was normal, karyotype was 46, XY, and diagnostic tests for Angelman, Pallister-Killian, Smith-Magenis, and Williams syndrome were negative. Family history was negative for WHSUS or CHH.

He was readmitted to the pediatric endocrine outpatient clinic at the age of 19 years due to delayed puberty. His bone age was 13 years and Tanner stage was G2P2 with testicular volume below 4 ml in the setting of low serum testosterone (<0.2 nM), LH (<0.1 IU/L) and inhibin B (40 ng/l) levels, findings consistent with hypogonadotropic hypogonadism. His TSH (2.89 mU/L), free t4 (11 pM), morning cortisol (264 nM), FSH (6.1 IU/L) and ACTH (22 ng/l) levels were normal. Thus, no signs of multiple pituitary hormone deficiency was noted. He detected strong odors.

At the age of 19 years and one month, puberty was induced with monthly intramuscular injections of testosterone (Sustanon®). The dose was gradually increased, and he masculinized normally (G4P4 at the age of 20 years), yet his testicular size remained constantly below 4 ml. After 24 months of testosterone treatment, his LH level was increased to 4.6 IU/L and FSH 16.7 IU/L, yet inhibin B level remained below 40 ng/l.

Genetic analyses

The genomic DNA was extracted from peripheral blood leukocytes. Whole Exome Family Plus Test was performed in an accredited genetic testing company (Blueprint Genetics, Helsinki, Finland). In brief, the test targets all protein-coding exons, exon-intron boundaries (± 20pbs) and selected non-coding, deep intronic variants. Sequencing was performed using the Illumina sequencing system with paired-end sequencing (150 by 150 bases). Sequencing-derived raw image files were processed using a base-calling software (Illumina) and the sequence data was transformed into FASTQ format. Sequencing yielded a 99% 20x coverage from all family members. Reads were mapped to the human reference genome (GRCh37/hg19). Burrows-Wheeler Aligner (WA-MEM) software was used for read alignment. Duplicate read marking, local realignment around indels, base quality score recalibration and variant calling were performed using GATX algorithms (Sentieon). Raw sequence reads were processed into variants by a

proprietary bioinformatics pipeline. Copy number variations (CNVs), defined as single exon or larger deletions or duplications (Del/Dups), were detected from the sequence analysis data using a proprietary bioinformatics pipeline, which processes aligned sequence reads. Blueprint Genetics variant classification follows the Blueprint Genetics Variant Classification Schemes modified from the ACMG guideline 2015.

In addition, to examine the presence of potentially causative variants in the genes implicated in CHH including the most recently discovered genes (n=75, Supplementary file 4) the patient's and the family members' vcf files from whole exome sequencing were annotated in-house using ANNOVAR (34). For a variant to be potentially causative we determined that the variant should be (i) be either exonic and nonsynonymous, or lie in the consensus splice site or its proximity, which we defined as within ten bases from the splice site, (ii) have a reported minor allele frequency (MAF) equal to or below 2% in all subpopulations in the gnomAD. Variants fulfilling these criteria were classified according to the ACMG/AMP 2015 guidelines using the InterVar bioinformatics software tool (35, 36).

Human pluripotent stem cells

H9 Human embryonic stem cell (hESC) (WA09; WiCell) (37) based H9C11 *GNRH1*-Tdtomato reporter cell line (Lund et al., 2016) was used to create H11, the *POGZ* patient mutation line carrying the heterozygous *POGZ* (c.2857C>T, p.(Gln953*)) mutation; and F6del, the *POGZ* deletion line with a 103bp deletion in *POGZ* exon19 (*POGZ*c.2803-2906del; p.E935Kfs*7). All the cell lines were maintained in Matrigel-coated dishes (Corning), using mTeSR1 culture medium (STEMCELL Technologies) at 37°C and 5% CO_2.

CRISPR/Cas9 editing

CRISPR single-guide RNAs (sgRNA) and homology-directed repair (HDR) template targeting exon 19 of *POGZ* were designed using https://benchling.com/. For the heterozygous mutation (H11 line), an RNP complex consisting of a sgRNA, an HDR oligo containing the c.2857C>T mutation, and Cas9 nuclease was formed; and for the homozygous deletion, another RNP complex consisting of two sgRNAs 103bp apart from each other, targeting *POGZ* exon 19, and Cas9 nuclease was formed. H9C11 *GNRH1*-TdTomato reporter cells ($2x10^6$) (29) were electroporated with one of the RNP complexes using the Neon transfection system (ThermoFisher Scientific, 1100 V, 20 ms, 2 pulses) and maintained in mTesR1 containing 10μM ROCK Inhibitor (Selleckchem) and 10% CloneR (STEMCELL Technologies) (38). 48 h after the electroporation, the cells were single cell-sorted using SONY SH800z sorter and the colonies were screened with Eco720i digestion and PCR. We chose the last exon for the deletion because it is the largest exon with most of the functional domains, and a vast majority of WHSUS cases has truncated variants in this area (27). The deletion is predicted to escape nonsense-mediated decay and produce a truncated protein *in silico* (https://nmdprediction.shinyapps.io). We validated the genotypes of the H11 and F6del

lines by sequencing and Western blot. The sgRNAs and HDR templates are provided in Supplementary file 1. The cytogenetic study with G bands performed in AmbarLab Barcelona showed a chromosomic formula of 46, XX in all lines (WT, H11, F6del), in the 20 metaphases analyzed.

GnRH neuron differentiation

WT *GNRH1*-reporter line H9C11, heterozygous patient mutation line H11, and homozygous deletion line F6del were differentiated into GnRH neurons using our GnRH differentiation protocol (28). Briefly, at ~90% confluence the protocol begins with dual SMAD inhibition (39) using N2B27 medium supplemented with 2 µM Dorsomorphin (Selleckchem) and 10 µM SB431542 (Sigma) for ten days, followed by ten days of 100ng/ml FGF8b (Peprotech) treatment. Subsequently, neurons are treated with 20 µM DAPT (Selleckchem) every other day for 5 days.

Quantitative RT-PCR

RNA isolation was performed using Nucleospin RNA plus kit (Macherey-Nagel) and one µg of total RNA was reverse transcribed into cDNA using iScript cDNA Synthesis Kit (Bio-Rad). Quantitative PCR was performed using the primers listed in Supplementary file 2. Gene expressions were calculated using the $2^{-\Delta\Delta Ct}$ method by normalizing to Cyclophilin G (*PPIG*) expression.

Immunoblotting

All cells were lysed in RIPA buffer (ThermoFisher Scientific) supplemented with 1x protease and phosphatase inhibitors (ThermoFisher Scientific). Denturated proteins loaded into 4-12% SDS-PAGE gels (Bio-Rad). Subsequently, the proteins were transferred onto nitrocellulose membranes (ThermoFisher Scientific) and the membranes were blocked with 5% milk in 1x TBS-T at room temperature (RT) for 1 h. Primary antibody incubations were performed overnight at 4°C and secondary antibody incubations were performed at RT for 1 h. The primary and secondary antibodies are listed in Supplementary file 3. The signal was detected with ECL Western Blotting Substrate (ThermoFisher Scientific) and captured with ChemiDoc Imaging System (Bio-Rad).

Immunocytochemistry and microscopy

Cells were fixed in 4% paraformaldehyde for 20 min at RT. After permeabilization with 0.5% Triton-X in 1x PBS for 10 mins at RT, cells were incubated with BlockAid Blocking Solution (ThermoFisher Scientific) for 1 h at RT. Primary antibody incubations were performed overnight at 4°C and secondary antibody incubations were performed in the dark at RT for 1 h. All primary and secondary antibodies were diluted in the blocking solution. The primary and secondary antibodies used in this study are listed in Supplementary

file 3. Images were taken using Zeiss Axio Imager.Z2 upright epifluorescence wide-field microscope (Biomedicum Imaging Unit, Helsinki).

Proliferation assay

On day 15 of the differentiation, cells were split into a new Matrigel-coated 12-well plate using three wells for each line (WT, H11, and F6del) and kept overnight to attach at 37°C and 5% CO_2. The next day, the plate was placed into the Incucyte S3 and scanned at 6-hour intervals using the Standard Software (Essen BioScience v2021). After 72 hours, cell confluency for each time point was calculated by normalizing occupied area to that of the starting time (hour 0) using the basic analyzer tool. Proliferation experiments were repeated for four times.

Wound-healing assay

On day 16 of the differentiation, cells were split into a Matrigel-coated Essen Incucyte®ImageLock 96 well plate (Sartorius) using three wells for each line (WT, H11, and F6del). Wounds were generated using the Incucyte® 96-Well Woundmaker Tool (Essen BioScience) and the cells were placed into the Incucyte S3 and scanned at 4-hour intervals using the Scratch Wound Cell Migration & Invasion Assay (Essen BioScience v2021). After 36 hours, average relative wound density was calculated for each line by normalizing to the initial wound density using the Incucyte® Scratch Wound Analysis Software.

Neurite length and neurite branch points measurements

Cells were split into Essen ImageLock 96-well plate on day 20 of the differentiation. After neurons were formed and matured with DAPT treatment (Day23), the plate was placed in the Incucyte S3 and scanned at 6-hour intervals for 42 hours. Neurite lengths (mm/mm^2) and neurite branch points (per mm^2) were calculated using Neurotrack Analysis Software Module.

Ethics

Written informed consents were obtained from the family. The study was approved by the Ethics Committee of the Hospital District of Helsinki and Uusimaa and was conducted in accordance with the Declaration of Helsinki.

Statistical methods

One-way ANOVA and Tukey' s multiple comparisons test, and paired-t test were performed for qPCR data of neural progenitor cell (NPC) markers, and glutamatergic neuron markers, respectively. Area under curve (AUC) analysis was performed for confluence and relative wound density graphs and then one-way ANOVA and Tukey' s multiple comparisons test were performed for AUC values as well as the neurite length and neurite branch point values at the end of the differentiation. All the statistical tests were

performed using GraphPad Prism (v9.2). P-value less than 0.05 was accepted to indicate statistical significance.

RESULTS

Identification of a novel POGZ mutation in a patient with WHSUS and KS

In whole exome sequencing, a heterozygous *de novo* nonsense variant c.2857C>T p.(Gln953*) in *POGZ* (NM_015100.4) was identified in the patient and also confirmed by Sanger sequencing (Supplementary Fig.3) The variant was not present in the patient' s parents or brother. Maternity and paternity were confirmed based on Whole Exome Family sequencing data. The variant is not present in gnomAD database. It causes a premature stop codon and is predicted to produce a truncated POGZ protein (952 out of 1410 amino acids), as the variant is located in the last exon of *POGZ* and expected to escape nonsense-mediated mRNA decay (40). The variant is predicted to lead to complete loss of the DNA-binding domain and the transposase-derived DDE domain of POGZ and result in loss of protein function. This genetic finding confirmed the diagnosis of WHSUS in the proband.

One heterozygous variant in *NRP2* (c.838C>T, p.Pro280Ser, rs79750907), encoding neuropilin receptor-2, was discovered in the patient among the 75 genes that have been implicated in CHH/KS. This variant is also carried by the healthy mother, has not been described in any CHH/KS patients, but has been proposed to underlie lymphedema based on a small pedigree without reported reproductive phenotypes (41). The allele frequency is 0.0018, and according to InterVar and ACMG/AMP 2015 guideline (32, 33) the variant is classified as likely benign.

Generation and validation of POGZ mutation hESC lines

We generated two hESC lines carrying two different POGZ mutations in previously described GnRH-reporter line (29) using CRISPR/Cas9 genome editing (Fig.2A). Western blot for POGZ showed that the H11 line produced both a full-length protein and a truncated protein product caused by the heterozygous nonsense mutation, as expected (Fig.2A). The F6del line produced only the truncated protein (Fig.2A). Both H11 and F6del lines were positive for OCT4 pluripotency marker (Supplementary Fig.1A), and the expression level of *SOX2, OCT4,* and *NANOG* were similar to that of unedited WT cells (Supplementary Fig.1B).

POGZ homozygous deletion impairs proliferation and wound-healing capacity of neural progenitor cells

During the FGF8 stage of the GnRH neuron differentiation, NPC pool actively proliferates and forms neural rosettes. Thus, we investigated the proliferation rate of NPCs derived from H11, F6del, and WT lines. Live-

cell time-lapse imaging showed that WT and H11 lines proliferated similarly, whereas the proliferation rate of the F6del NPCs was significantly lower (Fig.3A-B) ($p<0.005$).

We observed reduced migration of F6del neural progenitors in a wound healing assay by measuring the relative wound density (RWD) (42). It indicates the ratio of the occupied area to the total area of the initial wound region. 36 hours after the wound was made, RWD graph showed that WT and H11 lines closed more than 80% of the gap, however, F6del line was only able to close less than 50% (Fig.3C-D) ($p<0.05$).

POGZ homozygous mutation disrupts the formation of neural progenitor pool

Using our well-established GnRH neuron differentiation protocol (28), we differentiated WT, H11, and F6del lines into GnRH neurons. First, we produced *PAX6* and *FOXG1* expressing NPCs. *POGZ* knockout hESC lines reportedly have reduced number of intermediate progenitors (TBR1+ and TBR2+ cells) (24). Concordantly, we found significantly reduced expression of *TBR1* and *TBR2* ($p<0,0001$) together with markers of immature neurons *PAX6* ($p<0.01$) and *TUBB3* ($p<0.05$) in d15 neural progenitors derived from the F6del line (Fig.4).

POGZ mutant hESCs can differentiate to GnRH-expressing neurons but display reduced expression of glutamatergic neuron markers

GnRH differentiation protocol (Fig.5A) mostly produces excitatory glutamatergic neurons that express *TBR1*, and *LHX* family genes together with GnRH neurons (31). Tdtomato-positive, GnRH-expressing cells normally start emerging between d23-d25 of differentiation (28). By d25, TdTomato-positive cells were visible in all lines (Fig.5C). However, in line with the reduced proliferation of the NPCs, the number of neurons formed from the F6del line was clearly reduced compared to WT and H11 lines (Fig.5C). There were no significant differences in the *GNRH1* expression levels among the lines (Fig.5B). However, expression of the glutamatergic neuron markers *LHX2* and *TBR1* was significantly downregulated in the F6del line (Fig.5D).

Full-length POGZ is required for neurite outgrowth and branching

Neurite outgrowth and branching are fundamental parts of neuronal maturation (43). To assess the consequences of the *POGZ* mutations on anterior neurons including GnRH neurons we performed real-time measurements of neurite outgrowth and branching. During neuronal maturation under DAPT treatment, F6del neurons had significantly shorter neurites which grew significantly less than those of WT and H11 neurons (Fig.6A). The average neurite length of F6del neurons were 50% shorter compared to WT and H11 neurons on differentiation day 25 (Fig.6B) ($p=0.0002$).

Additionally, we examined neurite branching and observed that significantly fewer neurite branch points were formed in F6del neurons compared to WT and H11 (Fig.6C). At the end of the differentiation, F6del neurons had 90% less branch points than those of the WT and H11 neurons (Fig.6D) (p=0.0002).

DISCUSSION

POGZ is one of the most recurrently *de novo* mutated genes in patients with neuropsychiatric and neurodevelopmental disorders (NDDs) such as schizophrenia, intellectual disability, and ASD (19, 44). *POGZ* is highly expressed in the human fetal and adult central nervous system (CNS) (24) and, in mice, *Pogz* knockout is embryonic lethal (21, 45). So far, 50 disease-causing *POGZ* mutations have been reported in the HGMD database (HGMD Professional 2021.4). Stessman *et al.* reported 25 loss-of-function variants and three missense mutations in *POGZ* causing WHSUS and ASD, all of which occurred *de novo* (19). However, the function of POGZ during brain development and the role of *POGZ* mutations in the etiology of NDDs are largely unknown.

Here, we describe a White-Sutton syndrome patient with a novel heterozygous *de novo POGZ* mutation, and KS. In addition to WHSUS, he had a history of micropenis, incomplete puberty after the age of 18 years in the setting of low testosterone and gonadotropin levels, and absence of olfactory bulbs, *i.e.* findings consistent with KS (3). Indeed, WHSUS patients actually may harbor CHH/KS features such as olfactory bulb hypoplasia (46), midline defects (25, 47, 48), hypoplastic scrotum, hypoplastic testes, micropenis (27), and cryptorchidism (49), suggesting overlap between WHSUS and CHH/KS. Moreover, a very recent study by Oleari et al. reported that loss-off-function variants in another autism-linked gene, neuroligin 3 (*NLGN3*), may also be a rare cause of GnRH hormone deficiency (50). *NLGN3* is upregulated in maturing GnRH neurons and promotes neuritogenesis. Patients with *NLGN3* mutations presented with both ASD-features and GnRH deficiency phenotypes such as micropenis and small testes volumes, laying further credence to common genetic mechanisms underlying neurodevelopmental disorders such as GnRH deficiency and ASD (50).

During testosterone treatment to induce puberty, the patient' s gonadotropin levels increased, yet testis size remained small and serum inhibin B level low, arguing against extreme form of constitutional delay of growth and puberty or reversal of CHH (51). Interestingly, *POGZ* is expressed in spermatogonia and developing spermatogenic cells (https://www.proteinatlas.org/), and we cannot rule out the possibility that POGZ deficiency causes partial testicular resistance to gonadotropins, as described in approximately 10% of CHH patients (52).

We next sought after the putative mechanism by which POGZ defect might cause central hypogonadism. We differentiated POGZ-deficient hESC lines to GnRH neurons to bring the cells to NPCs that are further primed to GnRH neurons (28). Even the cell line carrying biallelic nonsense mutation in *POGZ* retained the capacity to be differentiated into GnRH neurons, suggesting that *POGZ* is not indispensable for GnRH neurogenesis. However, *Pogz* is highly expressed in rat embryonic GnRH neurons (50), and Burger et al. demonstrated *Pogz* enrichment in postnatal mouse GnRH neurons (53). In humans, Single Nucleus Pituitary Atlas (http://snpituitaryatlas.princeton.edu/) indicates *POGZ* expression in several types of pituitary cells both in pediatric and adult individuals. Finally, we now show POGZ expression in the GnRH neuron stage of our differentiation protocol (Supplementary Fig.2). In addition, a more global effect of *POGZ* deficiency on neurogenesis, rather than a specific problem of GnRH neuron ontogeny, is expected based on the wide neurological phenotype of WHSUS patients (25, 26, 27, 46, 47, 54).

Recently, two studies showed that loss of POGZ alters transcriptional networks underlying neuronal development, disrupts NSC proliferation, delays neuronal migration and neural induction of hESCs (23, 24). Similarly, we observed that homozygous deletion of *POGZ* leads to impaired proliferation and wound-healing capacity of NPCs, accompanied by downregulation of *PAX6, TBR1*, *TBR2,* and *TUBB3*. PAX6 is a key regulator of the neuronal fate determination as well as the self-renewal of the NSCs, and essential in the dorso-ventral patterning of the forebrain (55-58). T-box transcription factors *Tbr1* and *Tbr2* are expressed in the developing telencephalon, in the intermediate progenitor cells and in the dividing NPCs that give rise to olfactory bulb neurons (59). Their misexpression alters neuronal development, disrupts neuronal migration and dendrite development (60, 61). Mutations in *TUBB3*, encoding βIII-tubulin, an immature neuron marker and cytoskeletal regulator expressed in NPCs, lead to migration and axon guidance defects in CNS neurons (62-64), and are implicated in neurological disorders (65). Interestingly, the TUBB3 E410K syndrome overlaps with KS (17). Finally, the lack of full-length POGZ impaired neurite outgrowth and branching of anterior neurons, which is consistent with previous studies (21, 24, 66).

Of note, one copy of full-length POGZ was sufficient for the formation and expansion of the anterior NPCs and allowed generation of GnRH neurons. Indeed, heterozygous POGZ mutations apparently do not markedly disturb neuronal differentiation in vitro. For example, Deng et al. showed that an hESC line with a heterozygous POGZ mutation showed only subtle changes during neural differentiation (24). and Markenscoff-Papadimitriou et al. demonstrated a lack of strong transcriptional defects in developing human and mouse brain tissue with POGZ haploinsufficiency (67). Thus, the precise disease mechanism by which patients with POGZ mutation have WHSUS that overlaps with CHH/KS remains unclear (25-27) especially as oligogenecity could not be demonstrated.

In conclusion, our results suggest that *POGZ*, underlying WHSUS, is a rare cause of CHH/KS. Our results show that POGZ is not indispensable for GnRH neuron ontogeny, but is required for the proper proliferation of anterior NPCs, subsequent neurogenesis and axon branching of ensuing neurons, which may all contribute to the GnRH deficiency. Patients with WHSUS should be monitored for the onset of puberty and presence of hypogonadism to avoid adverse metabolic consequences of hypogonadism including osteoporosis.

Acknowledgements

We acknowledge Biomedicum Imaging Unit and Flow Cytometry Facility (University of Helsinki) for providing resources and services. We thank Kristiina Pulli for her support during the review of the manuscript.

Funding

This work has been funded by Academy of Finland (251413 and 275259 to T.R.), Sigrid Juselius Foundation (T.R.), Novo Nordisk Fonden (NNF17OC0027448 to T.R.), Foundation for Pediatric Research (T.R.), The Hospital District of Helsinki and Uusimaa/Children and Adolescents (T.R.), Instrumentarium Science Foundation (V.Y. and N.E.), The Paulo Foundation (N.E.), The Maud Kuistila Memorial Foundation (N.E.), Paivikki ja Sakari Sohlberg Säätio (V.Y.), and European Union' s Horizon 2020 research and innovation program under the HORIZON EUROPE Marie Sklodowska-Curie Actions grant agreement (894596 to Y.W, 813707 to S.M.)

Author Contributions

Conceptualization: N.E., Y.W. and T.R. Experiments: N.E., S.M., V.Y., and C.G-S. Data analysis: J.K., H.A. Writing-original draft: N.E. Writing-review and editing: N.E., K.V., Y.W., P.M., J.K., H.A., N.B., and T.R. Project Administration: N.E., T.R., K.V. Supervision: Y.W. and T.R. Funding acquisition: T.R.

Competing interests

The authors declare no competing or financial interests.

REFERENCES

1. Boehm U, Bouloux PM, Dattani MT, de Roux N, Dodé C, Dunkel L, et al. Expert consensus document: European Consensus Statement on congenital hypogonadotropic hypogonadism--pathogenesis, diagnosis and treatment. Nat Rev Endocrinol. 2015;11(9):547-64.

2. Balasubramanian R, Crowley WF, Jr. Isolated Gonadotropin-Releasing Hormone (GnRH) Deficiency. In: Adam MP, Everman DB, Mirzaa GM, Pagon RA, Wallace SE, Bean LJH, et al., editors. GeneReviews(®). Seattle (WA)1993.
3. Young J, Xu C, Papadakis GE, Acierno JS, Maione L, Hietamäki J, et al. Clinical Management of Congenital Hypogonadotropic Hypogonadism. Endocr. Rev. 2019;40(2):669-710.
4. Casoni F, Malone SA, Belle M, Luzzati F, Collier F, Allet C, et al. Development of the neurons controlling fertility in humans: new insights from 3D imaging and transparent fetal brains. Development. 2016;143(21):3969-81.
5. Cangiano B, Swee DS, Quinton R, Bonomi M. Genetics of congenital hypogonadotropic hypogonadism: peculiarities and phenotype of an oligogenic disease. Hum. Genet. 2021;140(1):77-111.
6. Barraud S, Delemer B, Poirsier-Violle C, Bouligand J, Mérol JC, Grange F, et al. Congenital Hypogonadotropic Hypogonadism with Anosmia and Gorlin Features Caused by a PTCH1 Mutation Reveals a New Candidate Gene for Kallmann Syndrome. Neuroendocrinology. 2021;111(1-2):99-114.
7. Chachlaki K, Messina A, Delli V, Leysen V, Maurnyi C, Huber C, et al. NOS1 mutations cause hypogonadotropic hypogonadism with sensory and cognitive deficits that can be reversed in infantile mice. Sci Transl Med. 2022;14(665):eabh2369.
8. Cotellessa L, Marelli F, Duminuco P, Adamo M, Papadakis GE, Bartoloni L, et al. Defective jagged-1 signaling affects GnRH development and contributes to congenital hypogonadotropic hypogonadism. JCI Insight. 2023;8(5).
9. Schnöll C, Krepischi ACV, Renck AC, Lima Amato LG, Kulikowski LD, Dantas NCB, et al. SIN3A defects associated with syndromic congenital hypogonadotropic hypogonadism: an overlap with Witteveen-Kolk syndrome. Neuroendocrinology. 2023.
10. Welch BA, Cho H-j, Ucakturk SA, Farmer SM, Cetinkaya S, Abaci A, et al. PLXNB1 mutations in the etiology of idiopathic hypogonadotropic hypogonadism. J. Neuroendocrinol. 2022;34(4):e13103.
11. Topaloglu AK, Simsek E, Kocher MA, Mammadova J, Bober E, Kotan LD, et al. Inactivating NHLH2 variants cause idiopathic hypogonadotropic hypogonadism and obesity in humans. Hum. Genet. 2022;141(2):295-304.
12. Whittaker DE, Oleari R, Gregory LC, Le Quesne-Stabej P, Williams HJ, Torpiano JG, et al. A recessive PRDM13 mutation results in congenital hypogonadotropic hypogonadism and cerebellar hypoplasia. J Clin Invest. 2021;131(24).
13. Chen Y, Sun T, Niu Y, Wang D, Liu K, Wang T, et al. Cell adhesion molecule L1 like plays a role in the pathogenesis of idiopathic hypogonadotropic hypogonadism. J. Endocrinol. Invest. 2021;44(8):1739-51.
14. Stamou MI, Georgopoulos NA. Kallmann syndrome: phenotype and genotype of hypogonadotropic hypogonadism. Metabolism: clinical and experimental. 2018;86:124-34.
15. Jongmans MC, van Ravenswaaij-Arts CM, Pitteloud N, Ogata T, Sato N, Claahsen-van der Grinten HL, et al. CHD7 mutations in patients initially diagnosed with Kallmann syndrome--the clinical overlap with CHARGE syndrome. Clin Genet. 2009;75(1):65-71.
16. Pingault V, Bodereau V, Baral V, Marcos S, Watanabe Y, Chaoui A, et al. Loss-of-Function Mutations in SOX10 Cause Kallmann Syndrome with Deafness. Am. J. Hum. Genet. 2013;92(5):707-24.
17. Chew S, Balasubramanian R, Chan WM, Kang PB, Andrews C, Webb BD, et al. A novel syndrome caused by the E410K amino acid substitution in the neuronal β-tubulin isotype 3. Brain. 2013;136(Pt 2):522-35.
18. Tata B, Huijbregts L, Jacquier S, Csaba Z, Genin E, Meyer V, et al. Haploinsufficiency of Dmxl2, encoding a synaptic protein, causes infertility associated with a loss of GnRH neurons in mouse. PLoS Biol. 2014;12(9):e1001952.
19. Stessman HAF, Willemsen MH, Fenckova M, Penn O, Hoischen A, Xiong B, et al. Disruption of POGZ Is Associated with Intellectual Disability and Autism Spectrum Disorders. Am J Hum Genet. 2016;98(3):541-52.

20. Ibaraki K, Hamada N, Iwamoto I, Ito H, Kawamura N, Morishita R, et al. Expression Analyses of POGZ, A Responsible Gene for Neurodevelopmental Disorders, during Mouse Brain Development. Dev Neurosci. 2019;41(1-2):139-48.
21. Matsumura K, Seiriki K, Okada S, Nagase M, Ayabe S, Yamada I, et al. Pathogenic POGZ mutation causes impaired cortical development and reversible autism-like phenotypes. Nat Commun. 2020;11(1):859.
22. Suliman-Lavie R, Title B, Cohen Y, Hamada N, Tal M, Tal N, et al. Pogz deficiency leads to transcription dysregulation and impaired cerebellar activity underlying autism-like behavior in mice. Nat Commun. 2020;11(1):5836.
23. Sun X, Cheng L, Sun Y. Autism-associated protein POGZ controls ESCs and ESC neural induction by association with esBAF. Mol Autism. 2022;13(1):24.
24. Deng L, Mojica-Perez SP, Azaria RD, Schultz M, Parent JM, Niu W. Loss of POGZ alters neural differentiation of human embryonic stem cells. Mol Cell Neurosci. 2022;120:103727.
25. Pascolini G, Agolini E, Fleischer N, Gulotta E, Cesario C, D'Elia G, et al. A novel patient with White-Sutton syndrome refines the mutational and clinical repertoire of the POGZ-related phenotype and suggests further observations. Am J Med Genet A. 2020;182(7):1791-5.
26. Merriweather A, Murdock DR, Rosenfeld JA, Dai H, Ketkar S, Emrick L, et al. A novel, de novo intronic variant in POGZ causes White-Sutton syndrome. Am J Med Genet A. 2022.
27. Assia Batzir N, Posey JE, Song X, Akdemir ZC, Rosenfeld JA, Brown CW, et al. Phenotypic expansion of POGZ-related intellectual disability syndrome (White-Sutton syndrome). Am J Med Genet A. 2020;182(1):38-52.
28. Lund C, Pulli K, Yellapragada V, Giacobini P, Lundin K, Vuoristo S, et al. Development of Gonadotropin-Releasing Hormone-Secreting Neurons from Human Pluripotent Stem Cells. Stem Cell Rep. 2016;7(2):149-57.
29. Lund C, Yellapragada V, Vuoristo S, Balboa D, Trova S, Allet C, et al. Characterization of the human GnRH neuron developmental transcriptome using a GNRH1-TdTomato reporter line in human pluripotent stem cells. Dis Model Mech. 2020;13(3):dmm040105.
30. Yellapragada V, Eskici N, Wang Y, Madhusudan S, Vaaralahti K, Tuuri T, et al. FGF8-FGFR1 signaling regulates human GnRH neuron differentiation in a time- and dose-dependent manner. Dis Model Mech. 2022;15(8).
31. Wang Y, Madhusudan S, Cotellessa L, Kvist J, Eskici N, Yellapragada V, et al. Deciphering the transcriptional landscape of human pluripotent stem cell-derived GnRH neurons: the role of Wnt signaling in patterning the neural fate. Stem Cells. 2022.
32. Andersson AM, Toppari J, Haavisto AM, Petersen JH, Simell T, Simell O, et al. Longitudinal reproductive hormone profiles in infants: peak of inhibin B levels in infant boys exceeds levels in adult men. J Clin Endocrinol Metab. 1998;83(2):675-81.
33. De Muinck Keizer-Schrama SM, Hazebroek FW, Drop SL, Degenhart HJ, Molenaar JC, Visser HK. Hormonal evaluation of boys born with undescended testes during their first year of life. J Clin Endocrinol Metab. 1988;66(1):159-64.
34. Wang K, Li M, Hakonarson H. ANNOVAR: functional annotation of genetic variants from high-throughput sequencing data. Nucleic Acids Res. 2010;38(16):e164.
35. Richards S, Aziz N, Bale S, Bick D, Das S, Gastier-Foster J, et al. Standards and guidelines for the interpretation of sequence variants: a joint consensus recommendation of the American College of Medical Genetics and Genomics and the Association for Molecular Pathology. Genet Med. 2015;17(5):405-24.
36. Li Q, Wang K. InterVar: Clinical Interpretation of Genetic Variants by the 2015 ACMG-AMP Guidelines. Am J Hum Genet. 2017;100(2):267-80.
37. Thomson JA, Itskovitz-Eldor J, Shapiro SS, Waknitz MA, Swiergiel JJ, Marshall VS, et al. Embryonic stem cell lines derived from human blastocysts. Science. 1998;282(5391):1145-7.
38. Balboa D, Weltner J, Novik Y, Eurola S, Wartiovaara K, Otonkoski T. Generation of a SOX2 reporter human induced pluripotent stem cell line using CRISPR/SaCas9. Stem Cell Res. 2017;22:16-9.

39. Chambers SM, Fasano CA, Papapetrou EP, Tomishima M, Sadelain M, Studer L. Highly efficient neural conversion of human ES and iPS cells by dual inhibition of SMAD signaling. Nat. Biotechnol. 2009;27(3):275-80.
40. Dyle MC, Kolakada D, Cortazar MA, Jagannathan S. How to get away with nonsense: Mechanisms and consequences of escape from nonsense-mediated RNA decay. Wiley Interdiscip Rev RNA. 2020;11(1):e1560.
41. Michelini S, Amato B, Ricci M, Kenanoglu S, Veselenyiova D, Kurti D, et al. Segregation Analysis of Rare NRP1 and NRP2 Variants in Families with Lymphedema. Genes (Basel). 2020;11(11).
42. Roddy M, Nelson T, Appledorn DM, Groppi V. IncuCyte® Scratch Wound 96-Well Real-Time Cell Migration and Invasion Assays. 2017.
43. Jin H, Kim B. Neurite Branching Regulated by Neuronal Cell Surface Molecules in Caenorhabditis elegans. Front Neuroanat. 2020;14:59.
44. Matsumura K, Nakazawa T, Nagayasu K, Gotoda-Nishimura N, Kasai A, Hayata-Takano A, et al. De novo POGZ mutations in sporadic autism disrupt the DNA-binding activity of POGZ. J Mol Psychiatry. 2016;4:1.
45. Gudmundsdottir B, Gudmundsson KO, Klarmann KD, Singh SK, Sun L, Singh S, et al. POGZ Is Required for Silencing Mouse Embryonic beta-like Hemoglobin and Human Fetal Hemoglobin Expression. Cell Rep. 2018;23(11):3236-48.
46. Garde A, Cornaton J, Sorlin A, Moutton S, Nicolas C, Juif C, et al. Neuropsychological study in 19 French patients with White-Sutton syndrome and POGZ mutations. Clin Genet. 2021;99(3):407-17.
47. Ferretti A, Barresi S, Trivisano M, Ciolfi A, Dentici ML, Radio FC, et al. POGZ-related epilepsy: Case report and review of the literature. Am J Med Genet A. 2019;179(8):1631-6.
48. White J, Beck CR, Harel T, Posey JE, Jhangiani SN, Tang S, et al. POGZ truncating alleles cause syndromic intellectual disability. Genome Med. 2016;8(1):3.
49. Murch O, Jain V, Benneche A, Metcalfe K, Hobson E, Prescott K, et al. Further delineation of the clinical spectrum of White–Sutton syndrome: 12 new individuals and a review of the literature. Eur. J. Hum. Genet. 2022;30(1):95-100.
50. Oleari R, Lettieri A, Manzini S, Paganoni A, André V, Grazioli P, et al. Autism-linked NLGN3 is a key regulator of gonadotropin-releasing hormone deficiency. Dis Model Mech. 2023;16(3).
51. Raivio T, Falardeau J, Dwyer A, Quinton R, Hayes FJ, Hughes VA, et al. Reversal of Idiopathic Hypogonadotropic Hypogonadism. N Engl J Med. 2007;357(9):863-73.
52. Sykiotis GP, Hoang X-H, Avbelj M, Hayes FJ, Thambundit A, Dwyer A, et al. Congenital Idiopathic Hypogonadotropic Hypogonadism: Evidence of Defects in the Hypothalamus, Pituitary, and Testes. J. Clin. Endocrinol. Metab. 2010;95(6):3019-27.
53. Burger LL, Vanacker C, Phumsatitpong C, Wagenmaker ER, Wang L, Olson DP, et al. Identification of Genes Enriched in GnRH Neurons by Translating Ribosome Affinity Purification and RNAseq in Mice. Endocrinology. 2018;159(4):1922-40.
54. Nagy D, Verheyen S, Wigby KM, Borovikov A, Sharkov A, Slegesky V, et al. Genotype-Phenotype Comparison in POGZ-Related Neurodevelopmental Disorders by Using Clinical Scoring. Genes (Basel). 2022;13(1).
55. Georgala PA, Carr CB, Price DJ. The role of Pax6 in forebrain development. Dev. Neurobiol. 2011;71(8):690-709.
56. Sansom SN, Griffiths DS, Faedo A, Kleinjan D-J, Ruan Y, Smith J, et al. The Level of the Transcription Factor Pax6 Is Essential for Controlling the Balance between Neural Stem Cell Self-Renewal and Neurogenesis. PLOS Genet. 2009;5(6):e1000511.
57. Wen J, Hu Q, Li M, Wang S, Zhang L, Chen Y, et al. Pax6 directly modulate Sox2 expression in the neural progenitor cells. NeuroReport. 2008;19(4):413-7.
58. Kallur T, Gisler R, Lindvall O, Kokaia Z. Pax6 promotes neurogenesis in human neural stem cells. Mol. Cell. Neurosci. 2008;38(4):616-28.

59. Bulfone A, Smiga SM, Shimamura K, Peterson A, Puelles L, Rubenstein JL. T-brain-1: a homolog of Brachyury whose expression defines molecularly distinct domains within the cerebral cortex. Neuron. 1995;15(1):63-78.
60. Crespo I, Pignatelli J, Kinare V, Méndez-Gómez HR, Esgleas M, Román MJ, et al. Tbr1 Misexpression Alters Neuronal Development in the Cerebral Cortex. Mol. Neurobiol. 2022;59(9):5750-65.
61. Hodge RD, Nelson BR, Kahoud RJ, Yang R, Mussar KE, Reiner SL, et al. Tbr2 Is Essential for Hippocampal Lineage Progression from Neural Stem Cells to Intermediate Progenitors and Neurons. J Neurosci. 2012;32(18):6275-87.
62. Moon HM, Wynshaw-Boris A. Cytoskeleton in action: lissencephaly, a neuronal migration disorder. Wiley Interdiscip. Rev. Dev. Biol. 2013;2(2):229-45.
63. Tischfield MA, Baris HN, Wu C, Rudolph G, Van Maldergem L, He W, et al. Human TUBB3 mutations perturb microtubule dynamics, kinesin interactions, and axon guidance. Cell. 2010;140(1):74-87.
64. Blumkin L, Leibovitz Z, Krajden-Haratz K, Arad A, Yosovich K, Gindes L, et al. Autosomal dominant TUBB3-related syndrome: Fetal, radiologic, clinical and morphological features. Eur. J. Paediatr. Neurol. 2020;26:46-60.
65. Poirier K, Saillour Y, Bahi-Buisson N, Jaglin XH, Fallet-Bianco C, Nabbout R, et al. Mutations in the neuronal β-tubulin subunit TUBB3 result in malformation of cortical development and neuronal migration defects. Hum. Mol. Genet. 2010;19(22):4462-73.
66. Zhao W, Tan J, Zhu T, Ou J, Li Y, Shen L, et al. Rare inherited missense variants of POGZ associate with autism risk and disrupt neuronal development. J Genet Genomics. 2019;46(5):247-57.
67. Markenscoff-Papadimitriou E, Binyameen F, Whalen S, Price J, Lim K, Ypsilanti AR, et al. Autism risk gene POGZ promotes chromatin accessibility and expression of clustered synaptic genes. Cell Rep. 2021;37(10):110089.

Figure Legends

Fig.1. Brain MRI scan of the proband at the age of 8 months. Sagittal T1 (left) and coronal T2 (right) images without contrast enhancement. Left panel, the pituitary gland is small (white long arrow). Neurohypophyseal bright tissue is seen in the normal localization (white short arrow). Right panel, Normal olfactory sulci are seen on both sides (black arrows). Olfactory bulbs were not visible on either side, although optimally located coronal slides are not available.

Fig.2. Generation and validation of POGZ mutation lines. Mutation lines H11 and F6del were derived from H9 GnRH-TdTomato reporter hESCs (Lund et al. 2020) using CRISPR/Cas9. The upper schematic displays the H11 line containing the heterozygous patient mutation (c.2857C>T, p. (Gln953*)) and the asterisk shows the heterozygous nucleotide change. The lower schematic displays the F6del line and the asterisk shows the homozygous premature stop codon. Protein schematic with POGZ Western blot analysis indicates that both lines produce truncated POGZ (HPZ: HP-1 binding zinc finger-like domain, CENP-B DB: centromere protein-B-like DNA binding domain, DDE: transposase-derived DDE domain).

Fig.3. POGZ homozygous deletion impairs proliferation and wound-healing capacity of neural progenitor cells. A. Cell proliferation rate was recorded from day 16 to day 19 of the differentiation from

the neural progenitor cells derived from WT, H11, and F6del lines. Cell confluences were normalized to the starting time point (0h). **B.** Overall proliferation of the F6del neural progenitors was significantly slower than that of WT and H11. The graph shows the area under the curve values of the confluence graph normalized to WT (n=4, **p<0.005). **C.** Relative wound density of all three lines between days 16 and 18 of the differentiation protocol. After 36 hours, WT and H11 cells almost completely closed the gap while the F6del clone was able to close only half of the same size gap within the same period of time. **D.** The graph shows the area under the curve values of the relative wound density graph normalized to WT (n=3, *p<0.5 **p<0.005)

Fig.4. POGZ homozygous deletion disrupts the formation of neural progenitor pool. Relative expression of early neuronal genes on day 15 of the differentiation was analyzed from neural progenitor cells derived from WT, H11, and F6del lines. F6del, the homozygous deletion clone, showed lower relative expression of intermediate progenitor neuron markers TBR1 and TBR2, and immature neuron markers PAX6 and TUBB3 (*: p<0.05, ***: p<0.01 ****: p<0,0001).

Fig.5. POGZ mutant hESCs can differentiate to GnRH-expressing neurons but display reduced expression of glutamatergic neuron markers. A. Schematic of the GnRH neuron differentiation protocol (Lund et al., 2020) that was used to differentiate WT, H11, and F6del lines into anterior neurons including GnRH neurons B. Relative GNRH1 expression was comparable among all three lines on day 25 of the differentiation. C. Day 25 images of WT, H11, and F6del lines at the GnRH stage of the differentiation. Arrows indicate the red *GNRH1*-expressing cells. D. The POGZ deletion clone F6del showed downregulation of glutamatergic neuron markers TBR1 and LHX2 on day 25 of the differentiation (*: p<0.05, ***: p<0.01).

Fig.6. Full-length POGZ is required for neurite outgrowth and branching. A. Neurite outgrowth of WT, H11, and F6del lines between days 23 and 25 of the differentiation protocol. B. The neurons derived from the F6del line had significantly shorter neurites compared to WT and H11 neurons on day 25. The graph shows the area under curve values of the neurite length graph (n=5, **p<0.0002). C. Neurite branch points of WT, H11, and F6del lines between days 23 and 25 of the differentiation protocol. D. The neurons derived from the F6del clone had significantly fewer branch points compared to WT and H11 neurons on day 25. The graph shows the area under curve values of the neurite branch points graph (n=3, p=0.0002).

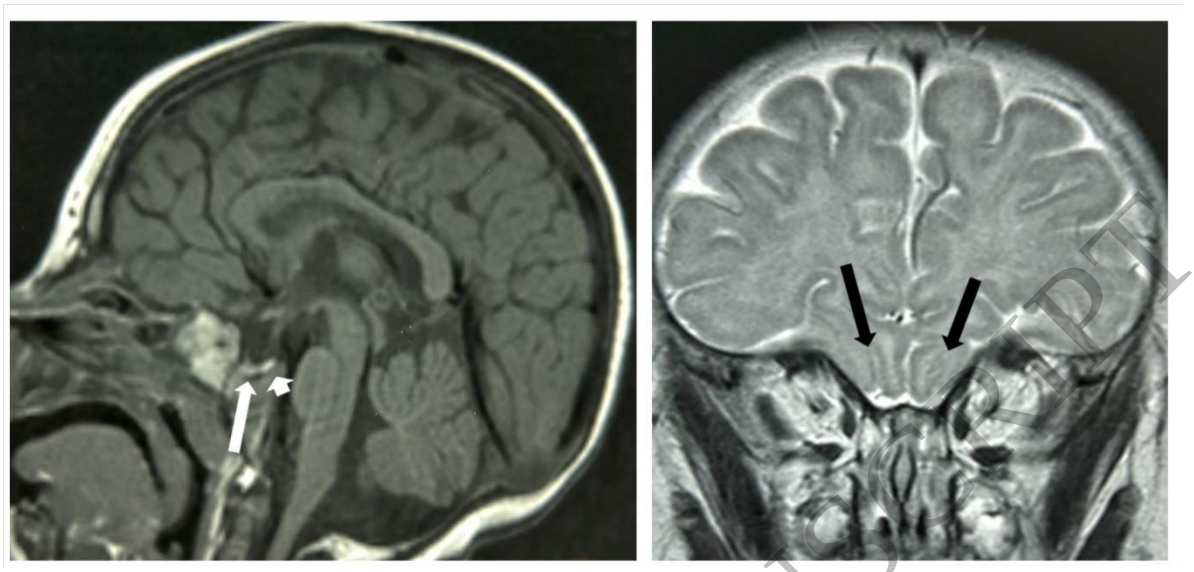

Figure 1
156x74 mm (x DPI)

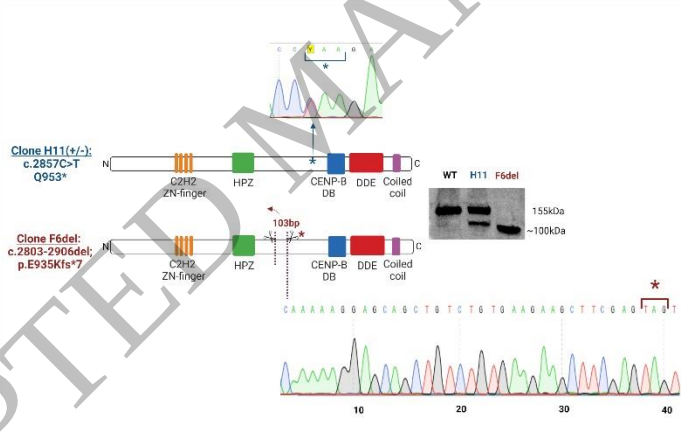

Figure 2
90x55 mm (x DPI)

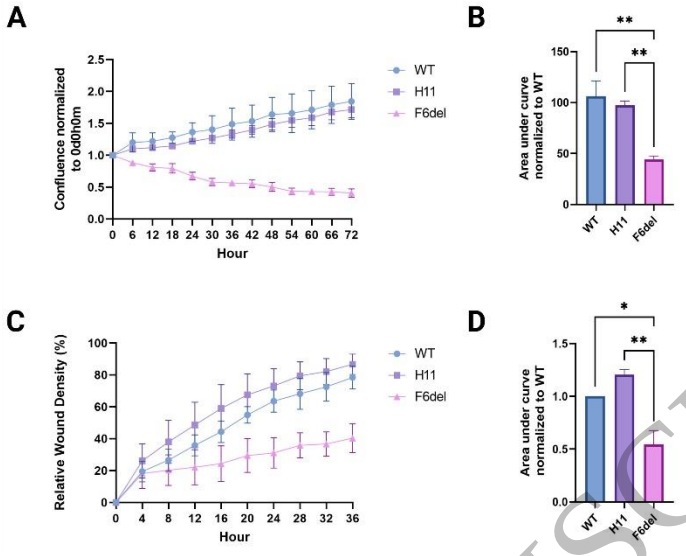

Figure 3
90x73 mm (x DPI)

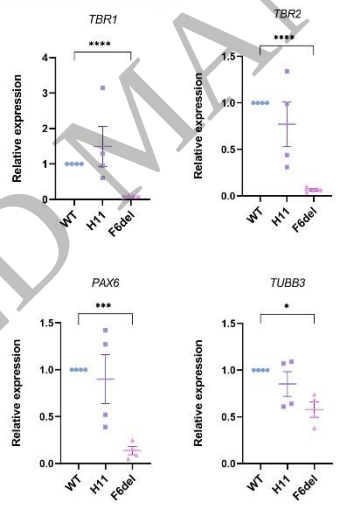

Figure 4
45x66 mm (x DPI)

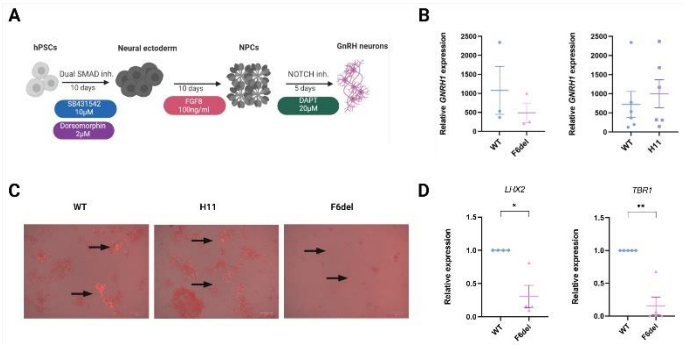

Figure 5
90x45 mm (x DPI)

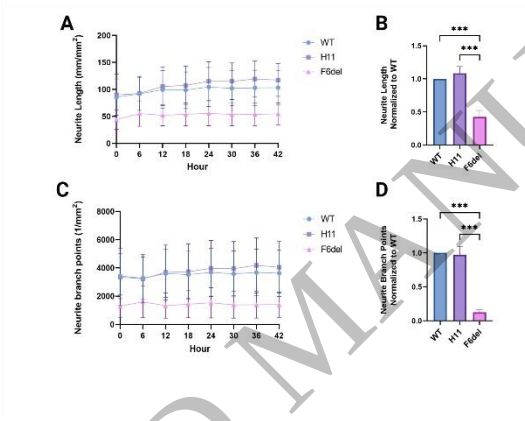

Figure 6
90x55 mm (x DPI)